First-Principles Molecular-Dynamics Study of Native Oxide Growth on Si(001)

Lucio Colombi Ciacchi and Mike C. Payne

Theory of Condensed Matter Group, Cavendish Laboratory, University of Cambridge, Cambridge CB3 0HE, United Kingdom

(Received 2 March 2005; revised manuscript received 1 August 2005; published 2 November 2005)

Through first-principles molecular dynamics we study the low-temperature oxidation of the Si(001) surface from the initial adsorption of an O_2 molecule to the formation of a native oxide layer. Peculiar features of the oxidation process are the early, spontaneous formation of Si^{4+} species, and the enhanced reactivity of the surface while the reactions proceed, until saturation is reached at a coverage of 1.5 ML. The channels for barrierless oxidation are found to be widened in the presence of both boron and phosphorous impurities.

DOI: 10.1103/PhysRevLett.95.196101 PACS numbers: 68.43.Bc, 71.15.Pd, 81.65.Mq, 82.65.+r

The chemical interactions between metals or semiconductors and the external environment are governed by a thin layer of oxide which spontaneously forms on their surfaces in contact with the atmosphere. This ''native oxide'' layer is responsible, for instance, for the biocompatibility and bioactivity of materials used in medical implantations [1]. Since silicon is increasingly regarded as a promising biomaterial [2], studying the formation of its native oxide becomes fundamental to understand the behavior of silicon devices under physiological conditions [3]. In general, Si surfaces are particularly sensitive to oxidation at room temperature, and to chemical attack by dioxygen dissolved in water solutions [4]. Moreover, the oxidation of silicon under wet conditions is related to the poorly understood mechanism of subcritical crack propagation in microelectromechanical devices [5]. Within this context, we carry out a thorough study of the formation of the native oxide layer on the Si(001) surface by performing a series of spin-unrestricted first-principles molecular-dynamics (FPMD) simulations within the density functional theory (DFT) formalism [6], using the Car-Parrinello (CP) method [7]. Our simulations (i) reveal a mechanism for the spontaneous dissociation of O_2 molecules during the oxidation reactions; (ii) naturally explain the formation of Si^{3+} and Si^{4+} species at oxygen coverages below 1 ML; (iii) show an enhanced reactivity of the surface while the oxidation takes place; and (iv) predict that the presence of boron and phosphorous dopants widens the channels for a barrierless oxidation process.

Because of its importance for the fabrication of electronic microdevices, the thermal oxidation of silicon has been widely investigated via a variety of experimental techniques (see, e.g., Ref. [8] and references therein). In contrast, investigations of the initial oxidation process at room temperature or lower are relatively rare [9,10]. As far as theoretical modeling is concerned, most existing studies have focused on static total energy calculations of oxide structures imposed *a priori* [11,12], or of the energy profile during the chemisorption of O_2 molecules along selected adsorption pathways [13,14]. Car-Parrinello molecular-dynamics simulations have been performed to study the interface between bulk silicon and its thermally grown oxide, as well as the reaction of oxygen molecules at the Si/SiO_2 interface [15,16]. The thermal growth of an oxide film on the Si(001) surface has been simulated via molecular-dynamics techniques either using large systems and classical potentials [17] or using an approximate DFT formalism and a simulation cell containing a single surface dimer [18]. The purpose of the present Letter is to study the spontaneous oxidation reactions at increasing oxygen coverage (i.e., using fairly large simulation cells) taking into account all the electronic degrees of freedom and allowing the spin of the system to evolve freely during the dynamics.

We start our study with a series of spin-unrestricted CP simulations of the chemisorption of an O_2 molecule on a $p(2 \times 2)$ reconstructed Si(001) surface [19]. In this structure, the undercoordinated Si atoms form rows of alternate ''up-down'' and ''down-up'' dimers, in which the ''up'' atom is higher above the surface than the ''down'' atom. This asymmetry is due to transfer of electronic charge from the down atom to the up atom (which gives the Si-Si bond some ionic character) and is the origin of a much more structured potential energy surface for O_2 adsorption than, for instance, on Al(111) [20]. Namely, when an O_2 molecule is placed at rest $\sim$3.2 Å above the surface, with the O-O axis parallel to the surface and perpendicular to the dimers direction [Fig. 1(a)], the molecule is initially repelled by the nucleophilic top atom of the nearest dimer [labeled T in Fig. 1(a)]. The molecule thus travels from its initial position above a dimer row toward the valley between two dimer rows, remaining at about the same distance from the surface [Fig. 2(a)]. After about 400 fs a spin-density cloud of opposite sign compared to the spin density associated with the unpaired electrons of O_2 localizes on the down atom of the dimer [labeled D in Fig. 1(a)], while a spin-density cloud of the other sign localizes on the top atom of a dimer nearby [Fig. 1(b)]. At this point the molecule rapidly binds to the surface, and its spin is quenched by electron donation from the surface to the π^* orbitals [Fig. 1(c)]. The molecule then spontaneously dissociates according to the same ''hot-atom'' mechanism that takes place during the chemisorption of O_2 on

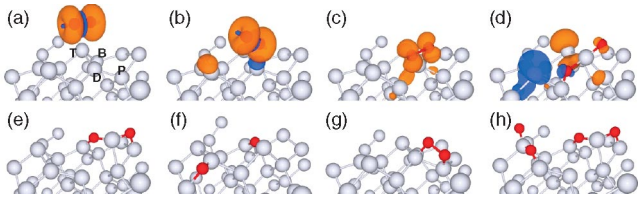

FIG. 1 (color). (a)–(e) Snapshots from a FPMD simulation of the dissociative chemisorption of O_2 (red atoms) on Si(001) (gray atoms). The spin density of the system at the values of 0.002 and −0.002 a.u. is depicted by the orange and blue isosurfaces, respectively. The atom labels in (a) are explained in the text. (f),(g) Final snapshots of two further simulations of the dissociative chemisorption process starting from different initial positions of the O_2 molecule. (h) Final snapshot of a simulation of the chemisorption of a second O_2 molecule on the surface shown in (e).

Al(111) [20], TiN(001) [1], and other metal surfaces [21]. After the dissociation, which induces a sudden increase in the local temperature up to ~550 K, spin-density clouds of different signs temporarily localize on the undercoordinated surface atoms [Fig. 1(d)], indicating a temporary increase of the surface reactivity while the chemisorption reaction proceeds. Eventually, the two O atoms remain trapped in a dimer site and in a backbone site, respectively, bound to the atom on which the molecule initially adsorbed [Fig. 1(e)]. We performed two further simulations of the same reaction, starting with O_2 over different sites and with different orientations with respect to the surface. Although the molecule is initially at rest in both cases, the simulations reveal a barrierless chemisorption pathway. In the second simulation O_2 again spontaneously dissociates [Fig. 1(f)]. Notably however, in the third simulation the molecule remains chemisorbed at a backbone site and does not dissociate within 1.6 ps [Fig. 1(g)]. Starting from this point we gradually increase the simulation temperature, until, after about 0.5 ps, the adsorbed molecule dissociates when the temperature reaches ~500 K. We therefore expect metastable adsorbed molecular precursors to be detectable on the surface only at very low temperatures, since phonons promote their dissociation, as in the case of Pt(111) [21].

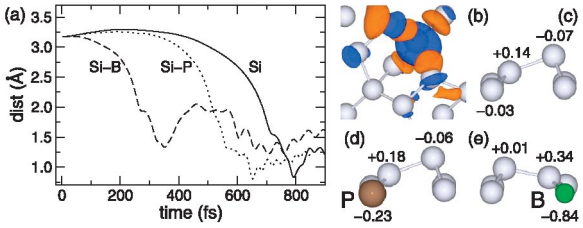

FIG. 2 (color). (a) Evolution of the distance between an O_2 molecule and the Si(001) surface during FPMD simulations of the chemisorption reaction in the absence of dopants (continuous line), in the presence of a subsurface phosphorous atom (dotted line), and in the presence of a subsurface boron atom (dashed line). (b) Charge-density difference between the surface with a P impurity in a subsurface site and the bare Si surface. Blue and orange isosurfaces represent positive and negative regions, respectively. (c),(d),(e) Mulliken charges of surface dimers of the bare surface, and in the presence of P and B subsurface impurities.

In contrast to the case of aluminum surfaces [20] but in agreement with previous findings [13], the barrierless oxygen chemisorption channels are quite narrow and the molecule undergoes considerable steering when navigating them. This is a consequence of the ionic character of the surface dimers which causes charge transfer from the surface to the O_2 molecule and orbital hybridization to compete with the electrostatic repulsion between the half-filled π^* orbitals of dioxygen and nucleophilic surface sites. It can be seen that the O_2 molecules readily bind to electron-deficient surface sites, such as the down atoms of the surface dimers. However, as revealed by the spin-density image [Fig. 1(c)] and confirmed by charge-density difference analysis, chemisorption still proceeds via electron donation from the surface into the antibonding π^* orbitals, which is made possible by the transfer of electrons of the opposite spin with respect to the unpaired electrons of O_2 from electron-rich Si atoms to the atoms closest to the molecule [see Fig. 1(b)].

The fact that two different processes, electron donation and bonding to electron-deficient sites, play a role in the dissociative chemisorption implies that impurities can change the rate of chemisorption by affecting either of these processes. When a phosphorous atom is placed in a subsurface site next to the down atom of a surface dimer [labeled P in Fig. 1(a)], the excess electron is strongly localized on the P atom, and only partially spreads on to the neighboring Si atoms [Fig. 2(b)]. Interestingly, there are zones of electron depletion located on the four bonds between the P atom and its next Si neighbors. Indeed, a Mulliken population analysis (using s and p atomic orbitals as the basis for the wave-function projection) reveals that the P atom receives electronic charge from the surrounding atoms [Fig. 2(d)]. In particular, the down atom of the next surface dimer becomes more depleted of electrons than it was in the absence of dopants. Therefore, while the charge transfer from the surface into the antibonding orbitals of an approaching O_2 molecule is expected to be enhanced by the presence of P, the electrostatic repulsion will not be increased, in spite of the excess electron. Indeed, when an O_2 molecule is placed in exactly the same position as in our first simulation [Fig. 1(a)], chemisorption proceeds faster than in the absence of dopants [Fig. 2(a)]. On the other hand, since the presence of electron-deficient sites also seems to favor the chemisorption process, it should also be facilitated by p dopants, such as boron atoms, which are known to preferentially segregate to surface or subsurface sites [22]. When a Si atom in the second surface layer [labeled B in Fig. 1(a)] is substituted with a B atom, after relaxation of the atomic positions the top-down dimer bound to the B atom changes configuration and becomes relatively flat. Analysis of the Mulliken charges shows that now both atoms of the dimer

are slightly positive, while electronic charge is donated into the boron site [Fig. 2(e)]. When an O_2 molecule is placed in the same position as in our first simulation [Fig. 1(a)] and the simulation in the presence of P, it is immediately attracted toward the surface and binds to it in less than 300 fs. Thus our simulations suggest that the channels for barrierless oxygen chemisorption are noticeably widened in the presence of both n and p dopants.

Following the simulations of the adsorption of a single O_2 molecule [Fig. 1(e)], we study the effect of increased oxygen coverage on further dioxygen chemisorption. When a second O_2 molecule is placed on top of a surface dimer with its O-O axis aligned along the dimer direction, it spontaneously adsorbs and dissociates [Fig. 1(h)]. A third molecule is then placed near the Si^{2+} atom generated in the first simulation. As the molecule approaches this atom, a spin-density cloud localizes on it [Fig. 3(a)], a first Si-O bond is formed, the molecule quickly adsorbs and then spontaneously dissociates upon filling of the σ^* antibonding orbital [Fig. 3(b)]. As a result of this hot-atom dissociation, the Si atom on which the molecule adsorbs is pulled out of the surface, while an O atom is temporarily pushed between the second and the third surface layers. A few hundred femtoseconds later this O atom moves up again and binds to the Si atom which has been pulled out of the surface. As a result, this Si atom ends up coordinated to four O atoms [Fig. 3(c)] and remains in this coordination for the rest of the simulation. Subsequently, we place two oxygen molecules about 2.7 Å above this surface and a new simulation is started. In this simulation, both molecules spontaneously adsorb and dissociate within 2 ps. Interestingly, after full relaxation of the atomic positions and minimization of the electronic structure, the system remains in a spin-unpaired electronic configuration with a large spin-density cloud localized on a threefold-coordinated Si atom [Fig. 3(d)]. In the next simulation, we place one O_2 molecule 3.4 Å above this threefold-coordinated Si atom, and a second O_2 molecule above another threefold-coordinated Si atom. While the first molecule immediately adsorbs on the spin-unpaired Si atom and dissociates, the second molecule does not absorb on the surface within 2.2 ps, at which point the simulation was stopped [Fig. 3(e)]. Notably, at the end of this simulation, two adjacent Si atoms remain threefold coordinated and separated by a distance of 3.0 Å [site A in Fig. 3(f)]. From this final configuration, we started a further dynamical simulation with one O_2 molecule initially 3.5 Å above this site, and a second O_2 molecule above a Si atom which is only coordinated to two O atoms [site B in Fig. 3(f)]. However, in this simulation neither of the O_2 molecules was able to find a pathway for spontaneous chemisorption. Indeed, analysis of the local density of states (LDOS) reveals that the HOMO and LUMO peaks around the twofold-coordinated Si atom are relatively distant from the Fermi level, which is consistent with a reduced reactivity at this site [Fig. 3(g), blue line]. For comparison, the LDOS around a reactive site [indicated with a red arrow in Fig. 3(d)] shows pronounced peaks just below and just above the Fermi level [Fig. 3(g), red line], while the LDOS around the atom coordinated by four oxygen atoms is very flat up to 3 eV below and above the Fermi level [Fig. 3(g), black line]. It appears that at oxygen coverages of about 1.5 ML there are either no channels, or very few very narrow channels for spontaneous oxidation. Remarkably, our simulations suggest that already at this low coverage there are no reactive sites present at the outer surface. In fact, reactive sites are situated at the interface between the bulk silicon and oxide layer [site A in Fig. 3(f)], but these will only become accessible to an incoming O_2 molecule after it overcomes the energy barrier associated with the repulsion between the negatively charged O atoms of the oxide and the O_2 molecule. These results are consistent with a medium-energy ion scattering study of the initial oxidation of Si(001) at room temperature, where the oxygen coverage has been found to saturate at 1.45 ± 0.05 ML [9].

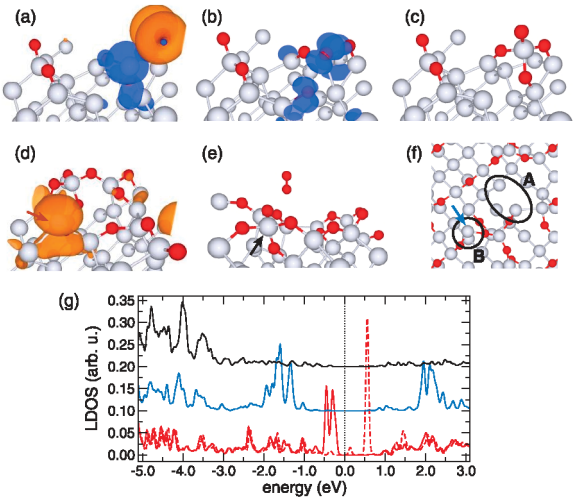

FIG. 3 (color). Same color code as in Fig. 1. (a)–(c) Snapshots from a FPMD simulation of O_2 chemisorption on the partially oxidized Si(001) surface shown in Fig. 1(h). (d)–(e) Final snapshots of further simulations of O_2 chemisorption at increasing oxygen coverage. (f) Top view of the final oxide structure showing sites where O_2 molecules were not observed to adsorb spontaneously. (g) LDOS around selected atoms indicated by arrows of the corresponding color in (d),(e), and (f). The solid and dashed lines correspond to the α and β spin manifolds.

The variation of the work function of the surface at increasing oxygen coverage is reported in Table I. Comparing these values with experiments is not trivial, due to the very limited size of our system. While experiments reveal a modest, monotonic increase of the work function upon oxidation [23], our calculations show quite an irregular pattern. It should be noted, however, that the strong electrostatic dipole due to the uncoordinated O atom bound to the Si^{4+} that has been formed [see Fig. 3(c)] is definitely responsible for the large $\Delta\phi$ computed at a coverage of 0.75 ML [24]. In a real system, local regions of high ϕ are probably compensated by other regions of low ϕ (for

TABLE I. Computed energy gain after O_2 chemisorption (ΔE) and variation of the work function ($\Delta\phi$) of the Si(001) surface at increasing oxygen coverages.

Coverage (ML)	0.00	0.25	0.50	0.75	1.00	1.25	1.50
ΔE (eV)	5.65	6.37	6.93	8.87[a]	8.87[a]	9.09	⋯
$\Delta\phi$ (meV)	0	−144	405	1480	⋯	94	116

[a]Average value per molecule in a simulation where two molecules react with the surface covered by 0.75 ML of oxygen.

instance, we compute a negative $\Delta\phi$ at a coverage of 0.25 ML), so that, on average, only a slight increase due to the formation of a thin oxide film is observed. Indeed, the average of all our $\Delta\phi$ values is 325 meV, which is consistent with the value of about 300 meV measured experimentally at coverages between 0.5 and 1 ML [23].

In the final structure obtained after simulating the chemisorption of a total of six O_2 molecules onto the silicon surface, 12 O atoms are bound to 13 Si atoms, forming 1 Si^{4+}, 1 Si^{3+}, 6 Si^{2+}, and 5 Si^{+} suboxide species. Despite the very limited size of the system and the very short simulation time, this composition is roughly consistent with the results of a synchrotron-radiation photoelectron spectroscopy study of the native oxide layer, where an almost Si-O stoichiometry and a distribution of species corresponding to 10% Si^{4+}, 14% Si^{3+}, 25% Si^{2+}, and 51% Si^{+} were found [9]. In particular, spectroscopic studies agree on the fact that Si^{3+} and Si^{4+} species appear at submonolayer coverages during the oxidation process at low temperatures [9,10]. We indeed observe that the adsorption of two oxygen molecules at the same site is sufficient to form an SiO_4 motif [Fig. 3(c)]. Interestingly, the reactivity of the surface appears to initially increase as the oxygen coverage increases. Namely, the channels for barrierless chemisorption are widened in the presence of adsorbed oxygen due to the formation of undercoordinated, electrophilic sites [see Figs. 3(a) and 3(d)]. In addition, we find that the energy gain from the reaction of O_2 with the surface increases with oxygen coverage (Table I), in part due to deep structural rearrangements of the oxide film, which help release its internal stress. Therefore, the initial oxidation process is both barrierless and, in a sense, "autocatalytic," and is hence expected to proceed via the fast formation of a large number of patchlike agglomerates of oxide species distributed randomly, as has been suggested on the basis of a number of experimental investigations [9,10].

The authors wish to thank M. Stengel and M. Galvan for valuable discussions. Computer time allocation has been provided by the Centre for High Performance Computing of the Dresden University, Germany, by the Cambridge-Cranfield High Performance Computing Facility, UK, and by the HPCx Consortium, UK. L. C. C. acknowledges support by the Alexander von Humboldt Foundation. This work is supported by the EPSRC under Grant No. GR/S61263/01.

[1] S. Piscanec *et al.*, Acta Mater. **52**, 1237 (2004).
[2] A. C. Richards Grayson, Proc. IEEE **92**, 6 (2004).
[3] G. Kotzar *et al.*, Biomaterials **23**, 2737 (2002).
[4] S. Watanabe and Y. Sugita, Surf. Sci. **327**, 1 (1995); H. Kanaya, K. Usuda, and K. Yamada, Appl. Phys. Lett. **67**, 682 (1995); C. P. Wade and C. E. D. Chidsey, Appl. Phys. Lett. **71**, 1679 (1997).
[5] C. L. Muhlstein, E. A. Stach, R. O. Ritchie, Acta Mater. **50**, 3579 (2002); H. Kahn, R. Ballarini, J. J. Bellante, and A. H. Heuer, Science **298**, 1215 (2002).
[6] M. C. Payne *et al.*, Rev. Mod. Phys. **64**, 1045 (1992).
[7] R. Car and M. Parrinello, Phys. Rev. Lett. **55**, 2471 (1985).
[8] H. Watanabe *et al.*, Phys. Rev. Lett. **80**, 345 (1998).
[9] Y. Hoshino *et al.*, Surf. Sci. **488**, 249 (2001).
[10] H. W. Yeom, H. Hamamatsu, T. Ohta, and R. I. G. Uhrberg, Phys. Rev. B **59**, R10 413 (1999).
[11] T. Yamasaki, K. Kato, and T. Uda, Phys. Rev. Lett. **91**, 146102 (2003).
[12] H. Kageshima and K. Shiraishi, Phys. Rev. Lett. **81**, 5936 (1998).
[13] K. Kato, T. Uda, and K. Terakura, Phys. Rev. Lett. **80**, 2000 (1998).
[14] X. L. Fan, Y. F. Zhang, W. M. Lau, and Z. F. Liu, Phys. Rev. Lett. **94**, 016101 (2005).
[15] A. Pasquarello and R. Car, Nature (London) **396**, 58 (1998).
[16] A. Bongiorno and A. Pasquarello, Phys. Rev. Lett. **93**, 086102 (2004).
[17] T. Watanabe, K. Tatsumura, and I. Ohdomari, Appl. Surf. Sci. **237**, 125 (2004).
[18] A. A. Demkov and O. F. Sankey, Phys. Rev. Lett. **83**, 2038 (1999).
[19] Our calculations are performed within the spin-polarized density functional theory using the PW91 exchange-correlation potential and norm-conserving pseudopotentials. The wave functions are expanded in plane waves up to a kinetic energy cutoff of 60 Ry, and a smearing of $k_BT = 0.1$ eV is applied to the electronic occupancies. A time step of 5.0 a.u. (~0.12 fs) is used in all dynamical simulations, which are performed at constant energy without any constraint on the simulation temperature, unless otherwise stated. The Si(001) surface is modeled with a periodically repeated slab of 8 Si layers separated by 8 corresponding layers of vacuum, using a 2×2 surface unit cell (which includes 8 surface atoms), and a 2×2 k-point distribution. The bare Si slab is $p(2 \times 2)$ reconstructed on both sides, and the bottom two Si layers are kept fixed in all dynamical simulations. The calculated equilibrium lattice parameter of bulk silicon is 5.457 Å.
[20] L. Colombi Ciacchi and M. C. Payne, Phys. Rev. Lett. **92**, 176104 (2004).
[21] J. Wintterlin, R. Schuster, and G. Ertl, Phys. Rev. Lett. **77**, 123 (1996).
[22] M. Ramamoorthy, E. L. Briggs, and J. Bernholc, Phys. Rev. B **59**, 4813 (1999).
[23] S. Surnev, Surf. Sci. **278**, 375 (1992).
[24] I. D. Baikie, U. Petermann, and B. Lägel, Surf. Sci. **433–435**, 770 (1999).